JMEPEG (2011) 20:40–47
DOI: 10.1007/s11665-010-9655-8

1059-9495/$19.00

Process Parameter Investigations of Backward Extrusion for Various Aluminum Shaped Section Tubes Using FEM Analysis

S. Orangi, K. Abrinia, and R. Bihamta

(Submitted August 3, 2009; in revised form March 9, 2010)

In this article, a FEM investigation has been carried out to analyze the backward extrusion of aluminum tubes which have internally and externally shaped sections. ABAQUS/Explicit finite element method was used to solve the problem. As a result, the distribution of stress, strain, and spatial velocity in the deformation region were obtained. Grid deformation patterns were also studied using the FE simulation to observe the material flow during the process. Initial billets with various cross sections such as rectangular, elliptical, hexagonal, octagonal, and square shapes were utilized in the simulations. Also various shaped punches such as circular and elliptical sections were employed for this analysis. In this article, the influence of the process parameters such as friction factor and reduction in area on the extrusion pressure was studied. The effects of reduction of area and friction factor on the configuration of free surface and velocity field have been investigated too. The results obtained from the present study were compared with analytical and experimental works and acceptable agreements were observed.

Keywords backward extrusion, FEM, shaped section aluminum tubes

1. Introduction

Industrial application of metal forming processes such as indirect extrusion has become increasingly popular. Detailed understanding of the material flow, stress and strain distribution, the influence of the process parameters such as friction, reduction of area, shape complexity factor, and other parameters on the extrusion pressure and the final product are very important.

In one of the analytical studies carried out on the indirect extrusion of shaped sections, Bae and Yang (Ref 1) presented an upper-bound solution for the final-stage extrusion load and the deformed configuration for the three-dimensional backward extrusion of internally elliptic-shaped tubes from round billets. Later on, Bae and Yang (Ref 2) using the upper bound analysis proposed a simple kinematically admissible velocity field for the backward extrusion of internally circular-shaped tubes from arbitrarily shaped billets. A new kinematically admissible velocity field was presented by Bae and Yang (Ref 3) to determine the final-stage extrusion load and the average extruded height in the backward extrusion of internally non-axisymmetric tubes from round billets.

Indirect extrusion of internally circular-shaped tubes from arbitrary shaped billets was presented by Lee and Kwan (Ref 4) in which a modified kinematically admissible velocity field was formulated. Lin and Wang (Ref 5) proposed a new upper-bound elemental method (UBET) for solving forging problems that were geometrically complex or needed a forming simulation for predicting the profile of the free boundary. Backward extrusion-forging of regular polygonal-shaped cup was analyzed by Moshksar and Ebrahimi (Ref 6) using an upper bound formulation. Finite element simulation was used to analyze axisymmetric hot backward extrusion problems by Guo et al. (Ref 7). A finite element simulation for the backward extrusion of internally hollow arbitrary shaped sections from arbitrary shaped billets was performed by Abrinia and Orangi (Ref 8-11).

In this article, backward extrusion of externally various shaped sections using finite element method was simulated to study the stress, strain, and velocity distribution in the deformation zone and to investigate effect of friction, area reduction, and shape complexity on the extrusion pressure.

2. FE Simulation

Simulation of backward extrusion of billets with initially shaped sections such as square, rectangle, ellipse, hexagon, and octagon, employing circular and elliptical punches were performed by ABAQUS/Explicit. AA2024-O and AA1100-O were chosen as the working materials.

In this simulation, billet dimensions for the AA1100-O were 22 mm width from side-to-side and 20 mm length (Ref 4) and for the AA2024-O, 25*25*2 mm (Ref 2). In the beginning of the process the distance between the punch and the billets was

S. Orangi, School of Mechanical Engineering, College of Engineering, University of Tehran, Tehran, Iran and Aluminum Research Centre (REGAL), Laval University, Quebec City, QC, Canada; **K. Abrinia**, School of Mechanical Engineering, College of Engineering, University of Tehran, Tehran, Iran; and **R. Bihamta**, Aluminum Research Centre (REGAL), Laval University, Quebec City, QC, Canada. Contact e-mails: Sakineh.orangi.1@ulaval.ca, cabrinia@ut.ac.ir, and reza.bihamta.1@ulaval.ca.

taken as 0.5 mm. The inside diameter of container in all cases was assumed to be 0.4 mm greater than that of billet. The 3D, C3D8R element used for the work piece, has eight nodes with reduced integration points which made it possible to endure higher amounts of deformation. In addition, friction factors for all simulations regarding AA1100-O were taken as 0.2 and for the AA2024-O, as 0.1 which were obtained experimentally in Bae and Yang (Ref 2) and Lee and Kwan (Ref 4), respectively, and implemented in simulation data. Therefore, it enabled the FE results to be compared with the experimental results (Ref 2, 4). The material model used in this study was isotropic and rigid-perfectly plastic. The material hardening curves have been shown in Fig. 1. Properties for the simulated models were assumed as follows:

For AA2024-O (Ref 2):

$$\bar{\sigma} = 292.77 \times \bar{\varepsilon}^{0.15}\,(\mathrm{MPa})$$

where $\rho = 2780$ (kg/m^3), $E = 73.1$ (GPa), $\nu = 0.33$, and $\sigma_y = 78.5$ (MPa).

And for AA1100-O (Ref 4):

$$\bar{\sigma} = 136 \times \varepsilon^{-0.254}(\mathrm{MPa})$$

where $\rho = 2715$ (kg/m^3), $E = 68.9$ (GPa), $\nu = 0.33$, and $\sigma_y = 34.5$ (MPa).

The area reduction defined as follows:

$$\mathrm{RA}\% = \frac{a}{A}(100)$$

where a is the section area of punch and A is the section area of billet.

Punch velocity is described as the displacement of punch per second and is given by:

$$\text{Punch velocity} = \frac{\text{displacement of the punch}}{\text{time step}}\left(\frac{\text{mm}}{\text{sec}}\right).$$

The gap between billet and container is neglected because the accuracy of calculations was 0.1 mm. Effect of this gap in area reduction is about 0.025-0.05 mm^2; thus it had no considerable influence on area reduction and was omitted in this equation.

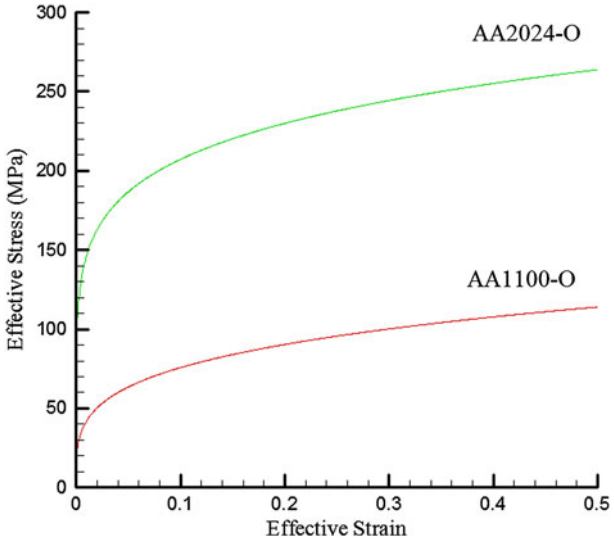

Fig. 1 Material hardening curves of AA2024-O and AA1100-O

Assumptions made in simulation were as follows:

(a) Material property for container and die were modeled as perfectly rigid.
(b) Interaction: tangential behavior with penalty formulation.
(c) Boundary conditions: container movement is constrained in all directions; punch movement was prevented in all directions except the vertical direction.
(d) Type of element for the container modeled as discrete rigid: R3D8R.
(e) Type of the element for punch modeled as analytical rigid: R3D4, a 4-node 3D bilinear rigid quadrilateral.
(f) Element type for billet modeled as deformable: C3D8R, an 8-node linear brick element.

The followings are meshing detail for extrusion of circular tube sections from rectangular billets:

1. The upper face of billet in contact with the punch was circularly partitioned.
2. Element shape: hexahedral with sweep technique.
3. Total number of nodes: 13416.
4. Total number of elements and their type: 12000 linear hexahedral elements of type C3D8R.
5. Element library: explicit, 3D stress.
6. In a lot of cases ALE adaptive mesh domain was used: re-meshing sweep per element: 500000, re-meshing sweep per increment: 3, initial re-meshing sweep value: 100.
7. In a few cases, distortion control was used in meshing control and the length ratio = 0.5 was chosen. This means the ratio of mesh length before distortion to the distorted length.

Element failure criteria: for all models, the optimum element size was obtained by trial and error until the appropriate aspect ratio = 3 were achieved.

3. Results and Discussion

3.1 Externally Square and Internally Circular Tubes

In Fig. 2 to 4, the simulation results for backward extrusion of square-shaped tubes from round billets have been illustrated. In Fig. 1 and 2, these results were compared with theoretical and experimental results of previous works, i.e., Bae and Yang (Ref 2), Lee and Kwan (Ref 4), and good agreement was observed.

3.1.1 Extrusion Load. Figure 2 illustrates the area reduction influence on the extrusion load in backward extrusion process of internally circular-shaped tubes from square billets. The extrusion load increases with increasing area reduction for a fixed aspect ratio and the given friction factor. Comparison of FE simulation with the experimental and theoretical values showed good agreement.

3.1.2 Relative Pressure. Comparing results of FE simulation, theoretical and experimental values of relative extrusion pressure for diverse area reductions in the extrusion of internally circular-shaped tubes from square billets have been presented in Fig. 3. With increasing area reduction for a given aspect ratio and friction factor, the rate of increase for the

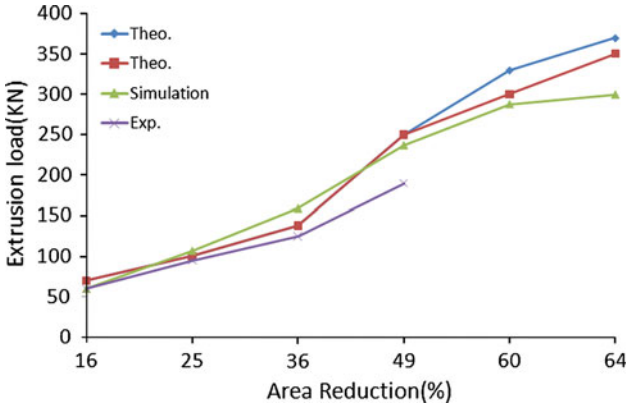

Fig. 2 Comparison of FEM simulation, theoretical and experimental extrusion loads of various area reductions for the extrusion of internally circular-shaped tubes from square billets, m = 0.1 (Ref 2, 4)

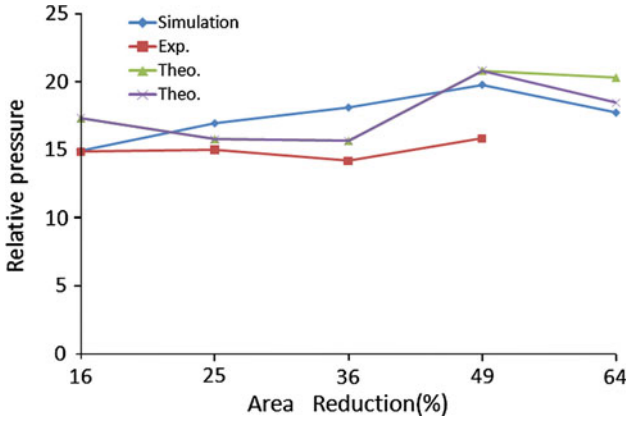

Fig. 3 Comparing of FEM simulation, theoretical and experimental relative pressures of diverse area reductions for the extrusion of internally circular-shaped tubes from square billets, m = 0.1 (Ref 2, 4)

relative extrusion pressure is lower than that of the extrusion load as shown in Fig. 2. This is because of the fact that with increasing area reduction, the area of the punch cross section increases thereby the division of force by area (pressure) reduces. The inverse happens in the case of forward extrusion because in forward extrusion, punch cross-sectional area is constant therefore the extrusion pressure increases with the same trend as the extrusion load. FE result was compared with the experimental and theoretical values and showed good agreements.

3.1.3 Stress Distribution and Grid Deformation. A stress distribution contour of the backward extrusion of circular tubes with square sections is indicated in Fig. 4 as FE simulation result. The Von-Mises stress increases from the center of the section toward the internal wall of work piece then it diminishes toward external wall. It seems that because of material flow under the punch and the frictional velocity discontinuities, the stress increases. However, as the material flow develops further toward the external surface it passes over the punch area and since there are no obstacle in the path of the material flow it decreases at this position. In the vertical direction of the deformation area and under the punch, the

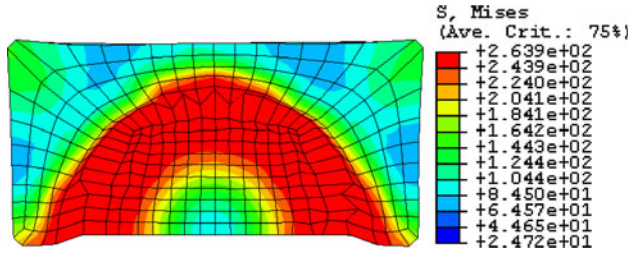

Fig. 4 Simulation results of stress distribution and grid deformation of internally circular-shaped sections from square billets, RA = 49%, AA2024-O, m = 0.1

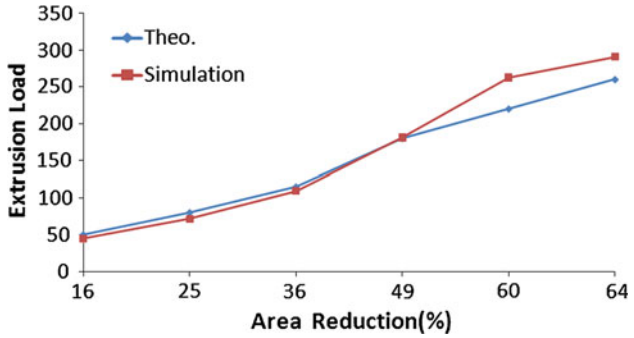

Fig. 5 FEM simulation results in comparison with theoretical extrusion loads of different area reductions for the extrusion of internally circular-shaped tubes from hexagonal billets, m = 0.1 (Ref 2)

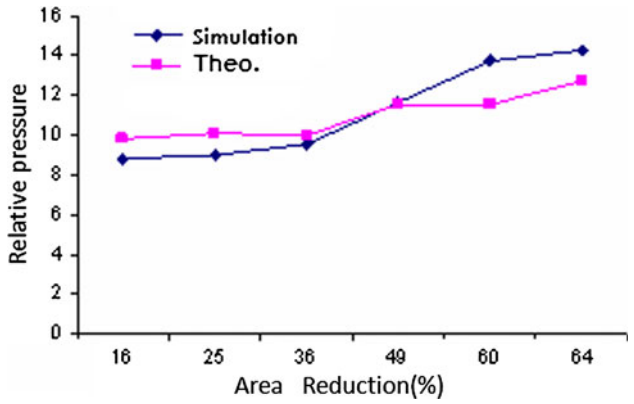

Fig. 6 Comparison of FEM simulation and theoretical relative pressures of diverse area reductions for the extrusion of internally circular-shaped tubes from hexagonal billets, m = 0.1 (Ref 2)

conical-shaped dead zone is created which acts rigidly and moves downward with the punch as if it was part of the punch.

3.2 Internally Circular and Externally Hexagonal Shape Extrusion

FE simulation results for backward extrusion of circular-shaped tubes from rectangular billets have been shown in the Fig. 5 to 9.

3.2.1 Extrusion Load. Figure 5 shows the effect of area reduction on the extrusion load for backward extrusion of internally circular-shaped tubes from hexagonal billets. With

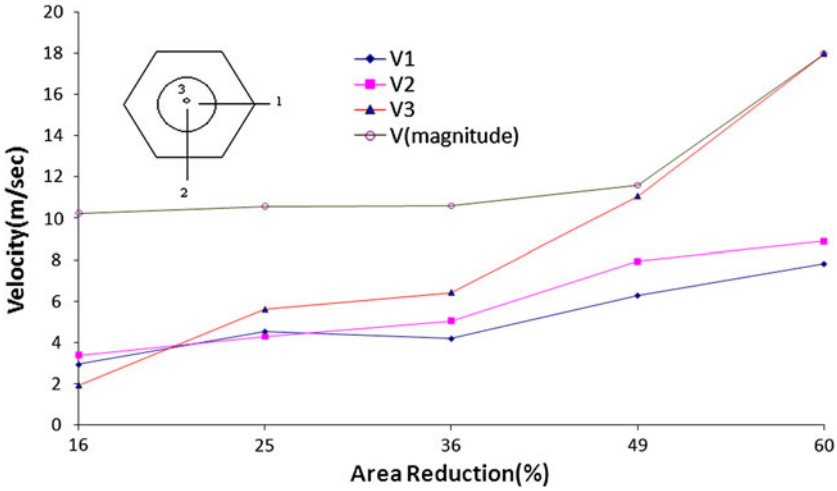

Fig. 7 Simulation outcome for area reduction influence on velocity field of hexagonal billet

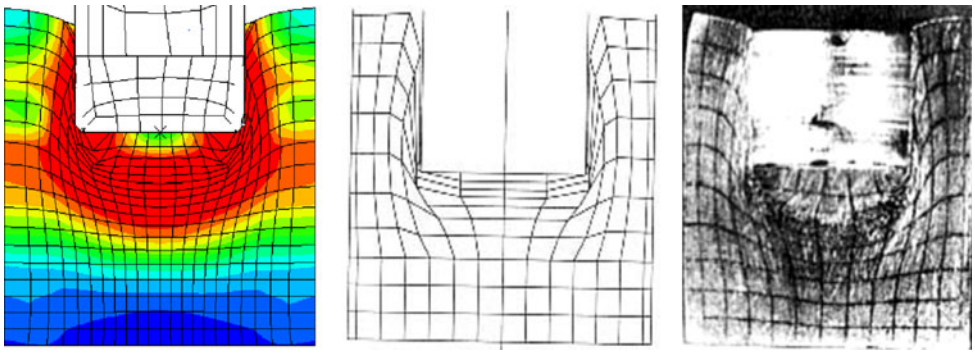

Fig. 8 Simulation results of grid deformation in comparison with theoretical and experimental results (Ref 4), RA = 35.6%, AA1100-O, m = 0.2, Left-to-right: simulation, theoretical, experimental results, respectively

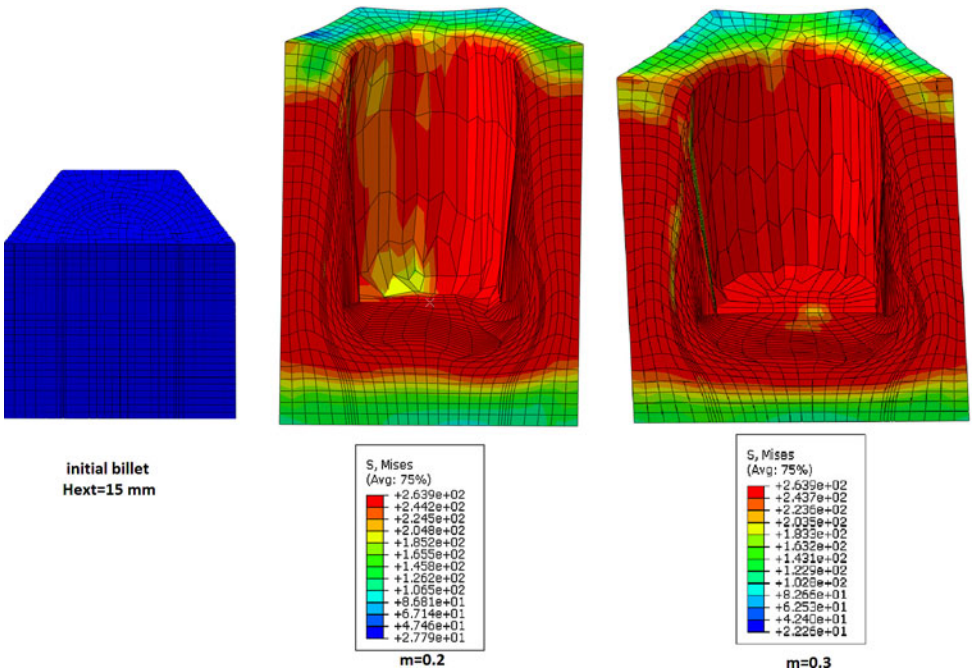

Fig. 9 Simulation results of the friction factor effect on the configuration of the free surface and velocity field distribution of internally round-shaped tubes from hexagonal billets, RA = 36%, hex. = 2.5

increasing area reduction, the extrusion load increases in constant aspect ratio and assumed friction factor. Good agreement was observed in comparing FE results with theoretical values (Ref 2).

3.2.2 Relative Pressure. A plot of relative extrusion pressure for internally circular and externally hexagonal-shaped tubes is shown in Fig. 6. Note that both FE simulation and presented upper bound theory (Ref 2) predict the same trend and the extracted results are close to each other too. As was the case for Fig. 3, with increasing area reduction, the rate of increase for the relative pressure is lower than that of extrusion load and the aspect ratio and frictional conditions were kept constant.

3.2.3 Distribution of Velocity and Configuration of the Free Surface of the Extruded Billet. The Simulation results for the influence of the reduction in area on the velocity field have been shown in Fig. 7. It could be observed that as the reduction in area increases from 16 to 49%, all three components of velocity (V1, V2, and V3) have similar magnitudes but at higher reductions the component V3 suddenly rises sharply. The reason for this seems to be the shape of the circular tube which is being extruded. At lower reductions, the thickness of tube walls is such that the flow of material happens evenly in all directions. However, at 60% area reduction, it is clear that the components of velocity in the directions (1) and (2) follow the same trend as before while the component of velocity in direction (3) increases with sharp trend. This phenomenon can be explained by thinning of extruded wall which causes faster flow of material in this direction.

3.2.4 Grid Deformation. To verify the grid deformation for the backward extrusion of internally circular-shaped tubes from hexagonal billets, Fig. 8 compares FE simulation results with experimental and theoretical results which presented in Lee and Kwan (Ref 4). FE outcomes are closer to the experimental results than the upper bound solutions. As illustrated in the figure, maximum deformation is observed in the corners and walls of the workpiece.

3.2.5 Effect of Friction Factor on the Free Surface Configuration. The influence of friction factor on the configuration of the free surface for a constant aspect ratio and area reduction is presented in Fig. 9. The gradient of Von-Mises stress in extrusions increases with increasing friction from 0.2 to 0.3.

3.3 Results of Backward Extrusion Process with Octagonal Billet and Circular Punch

Figures 10 to 12 present the results of FE simulation for the backward extrusion of internally circular sections from octagonal billets.

3.3.1 Extrusion Load. In Fig. 10 a graph of extrusion load versus area reduction is illustrated for the backward extrusion of internally circular sections from octagonal billets. Comparison of other theoretical results with the FE simulation of the authors is also presented in this figure. Author's results show good accordance with the theoretical values (Ref 2) for 16 to 60% of area reductions.

3.3.2 Relative Pressure. To compare simulation and theoretical results of relative pressures versus various area reductions, plots have been presented in Fig. 11. With increasing area reduction, the rate of increase for the relative pressure is lower than that of extrusion load as shown in this figure.

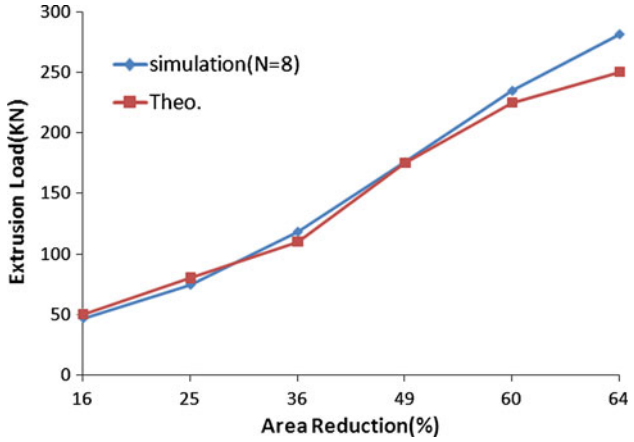

Fig. 10 FE simulation and theoretical extrusion loads comparison of different area reductions for the extrusion of internally circular-shaped tubes from octagonal billets, $m = 0.1$ (Ref 2)

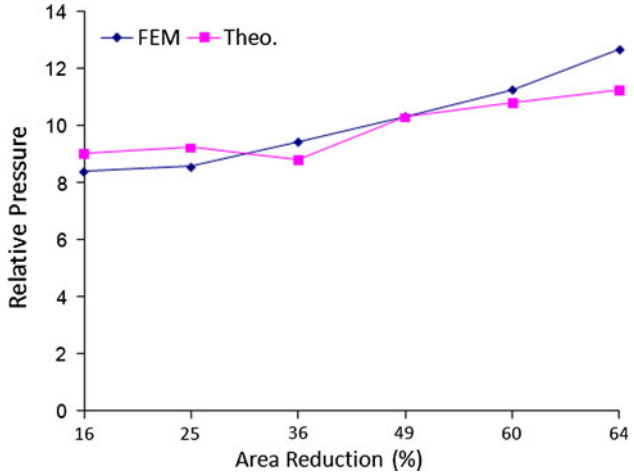

Fig. 11 Comparison of FE simulation and theoretical relative pressures vs. different area reductions for the extrusion of internally circular-shaped tubes from octagonal billets, $m = 0.1$ (Ref 2)

In all simulation instances like previous theoretical analysis aspect ratio and friction factor were kept constant. Good agreement is seen when comparing the simulation and theoretical results (Ref 2).

3.3.3 Velocity Distribution and the Effect of Area Reduction on the Free Surface Configuration. Effect of area reduction on the configuration of the free surface and velocity field contours of extruded billet for a certain aspect ratio and friction factor are shown in Fig. 12. Clearly, with an increase in the area reduction wall thickness of the extruded product reduces. Hence the height of the extruded tube becomes higher for higher reductions and that is why the maximum velocity is shown to increase in this simulation. Also, from Fig. 12 it could be concluded that for higher area reduction, the velocity contour spreads in a larger area in the material; therefore, the material moves freely due to lesser constraints around it. That is why thinner walls for the extruded products are more prone to distortion due to their more free movement.

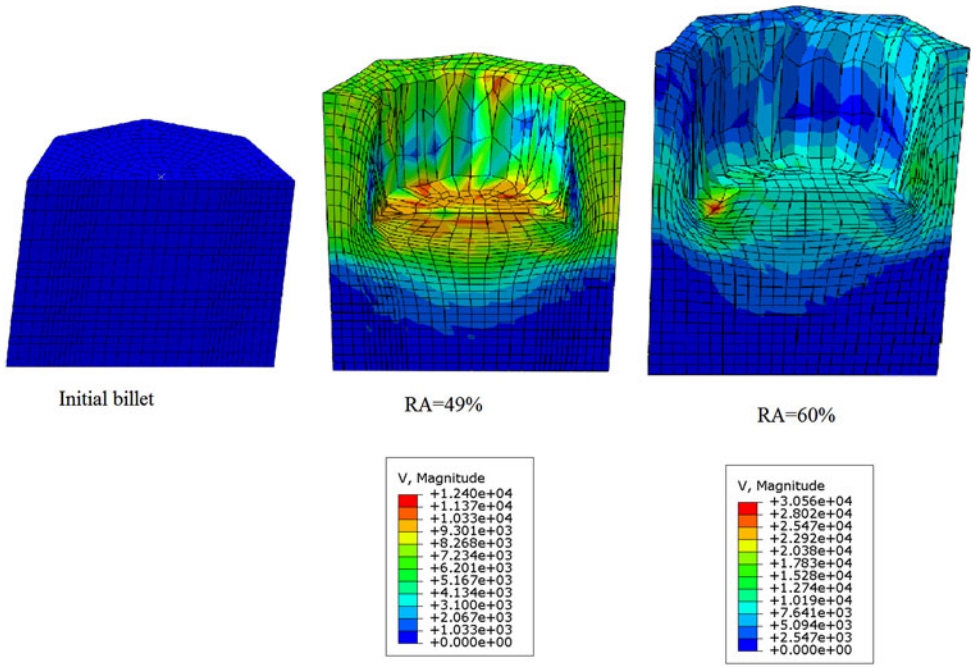

Fig. 12 Simulation results of area reduction influence on the configuration of the free surface and the velocity distribution of the extruded billet, $m = 0.1$, $N = 8$

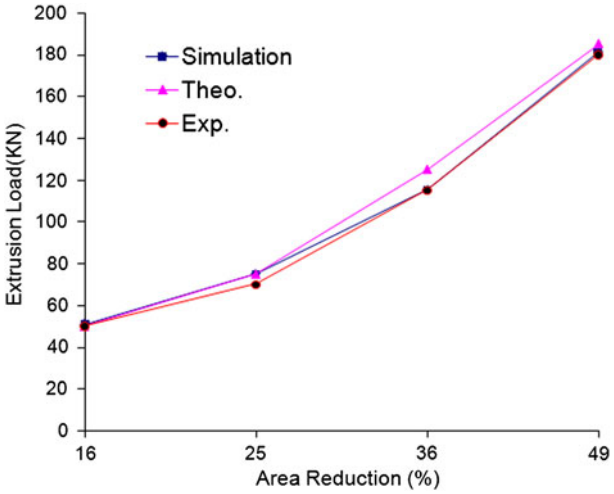

Fig. 13 Extrusion load variable vs. reduction of area for backward extrusion of internally round-shaped tubes from rectangular billets, $m = 0.1$, $a/b = 1.25$ (Ref 2, 10)

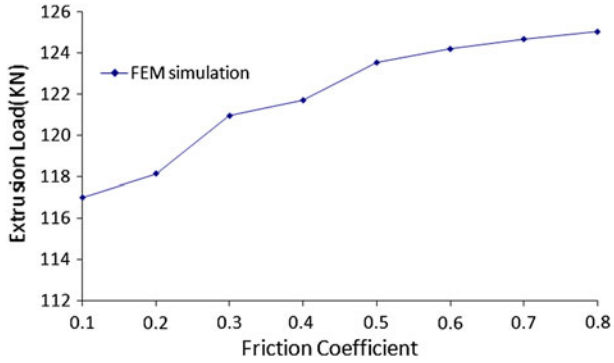

Fig. 14 Extrusion load variable vs. friction factor for backward extrusion of internally round-shaped tubes from rectangular billets (Ref 10)

3.4 Externally Rectangular and Internally Round-Shaped Tubes

Figures 13 to 16 depict the results of FE simulation for the backward extrusion of internally round sections from rectangular billets.

3.4.1 Extrusion Load. In Fig. 13, the effect of area reduction on the extrusion load has been depicted for backward extrusion of internally circular-shaped tubes from rectangular billets. The extrusion load goes up with increasing area reduction, for a certain aspect ratio and the friction factor. FE simulation method was compared with the experimental and theoretical values (Ref 2) and good agreements were observed.

3.4.2 Friction Factor. The diagram of extrusion load variations versus friction factors for the backward extrusion simulation of internally rectangular sections from circular billets is shown in Fig. 14. The extrusion load increases with increasing friction factor.

3.4.3 Strain Distribution. Four stages of backward extrusion process have been simulated in the Fig. 15. Plastic equivalent effective strain contours of internally circular and externally rectangular-shaped tubes are shown in this figure. It could be seen that, as expected, the highest values of strains occur at where the maximum deformation exists. The plastic equivalent effective strain in the areas where the work piece contacts the punch corners, is greater than elsewhere. Consequently, maximum deformation happens in the zone of the work piece in contact with the punch corner. In addition, in the initial stage of the process, contours of strains are distributed in broad areas and gradually decrease through the end of process. This is because, in the initial stage, with increasing stress, the plastic area develops and includes larger region of billet;

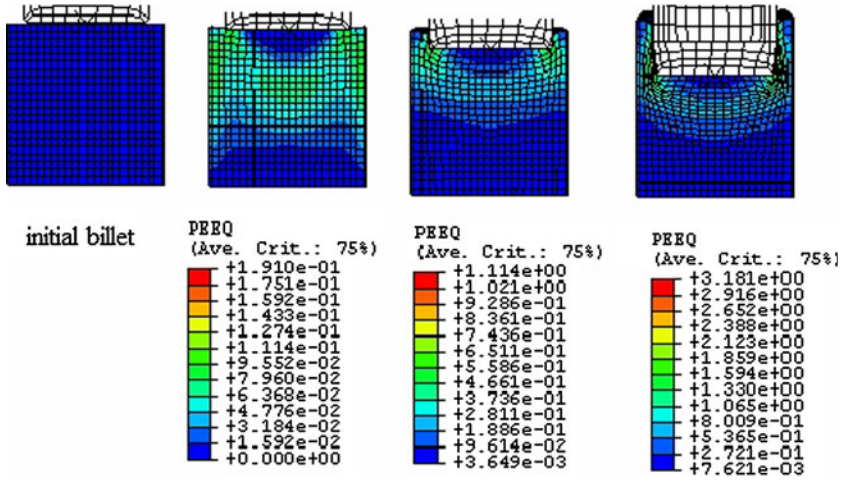

Fig. 15 Distribution of plastic equivalent strain in backward extrusion simulation of internally round shapes from square billets, RA = 49% (Ref 10)

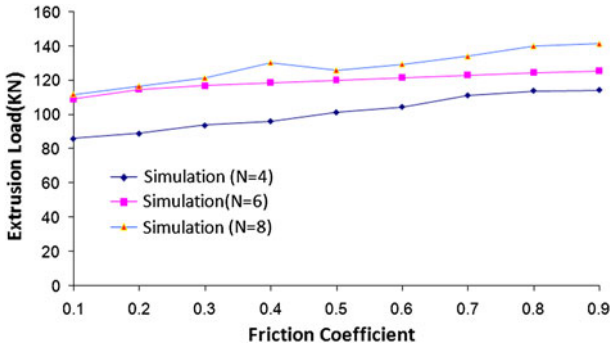

Fig. 16 Extrusion load variables vs. friction factor for round-shaped tubes from polygonal billets RA = 36%, AA2024-O

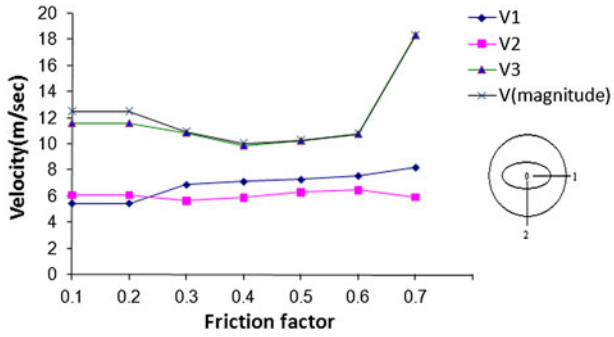

Fig. 17 Velocity variables vs. friction factor for internally elliptic-shaped tubes from elliptic billets

however, after material flows, there is no need for the load to increase and the deformation area is fixed and strains are confined to smaller plastic areas.

3.4.4 Extrusion Load Variables Versus Friction Factor for Polygonal Billets and Circular Punches. The results of FE simulation for backward extrusion of internally circular-shaped tubes from polygonal billets are depicted in Fig. 16 as the diagram of extrusion load versus friction factor. It could be concluded that with increasing number of polygonal edges, the extrusion load goes up. This is by virtue of increasing area of billet contacting with the container; hence, the friction force rises and causes an increase in the extrusion load.

3.5 Backward Extrusion of Elliptic-Shaped Tubes from Elliptic Billets

The simulation outcomes of backward extrusion process of elliptic-shaped tubes from elliptic billets are illustrated in Fig. 17 and 18.

3.5.1 Effect of Friction Factor on Velocity Field. In Fig. 17, effect of friction factor on the maximum velocity has been shown. For $m = 0.1$ to $m = 0.6$ no considerable difference among maximum velocities was observed.

3.5.2 Velocity Field Distribution. For the same extrusion, the grid deformation and spatial velocity distribution at nodes are also seen in Fig. 18. Starting from the initial stage of the extrusion process and going through to the end, five different stages are observed. The values of velocity distribution in the part are also shown for each stage. The velocity field is shown by three components. Considering stages (1) to (3) in Fig. 18, it could be seen that the velocity contour spread in the work piece and in stages (4) to (5) it is confined to the deformation zone. The reason for this could be explained by the fact that at the early stages of the process as the moving punch hits the stationary work piece, its impact is felt in most parts of material and as the process moves into more stable stages of deformation (4 and 5), the contours of the velocity distribution are limited to the region where material flow occurs.

The magnified figure of one stage for contour distribution of V1, V2, and V3 are illustrated in Fig. 18(I), (II), and (III). V1 was greater at locations near to the punch corner than elsewhere and it is minimum at the center of free surface of extruded part (1). Also V1 decreases from nodes (1) to (2), near the wall of the container.

V2 was greater at locations (3), (4), and between these sections, V2 is the lowest. Velocity component V3 was the greatest at (5) and decreases toward (6), work piece nodes near the container wall. From (7) near free surface of work piece, toward (8), nodes near container lower section, V3 decreases gradually.

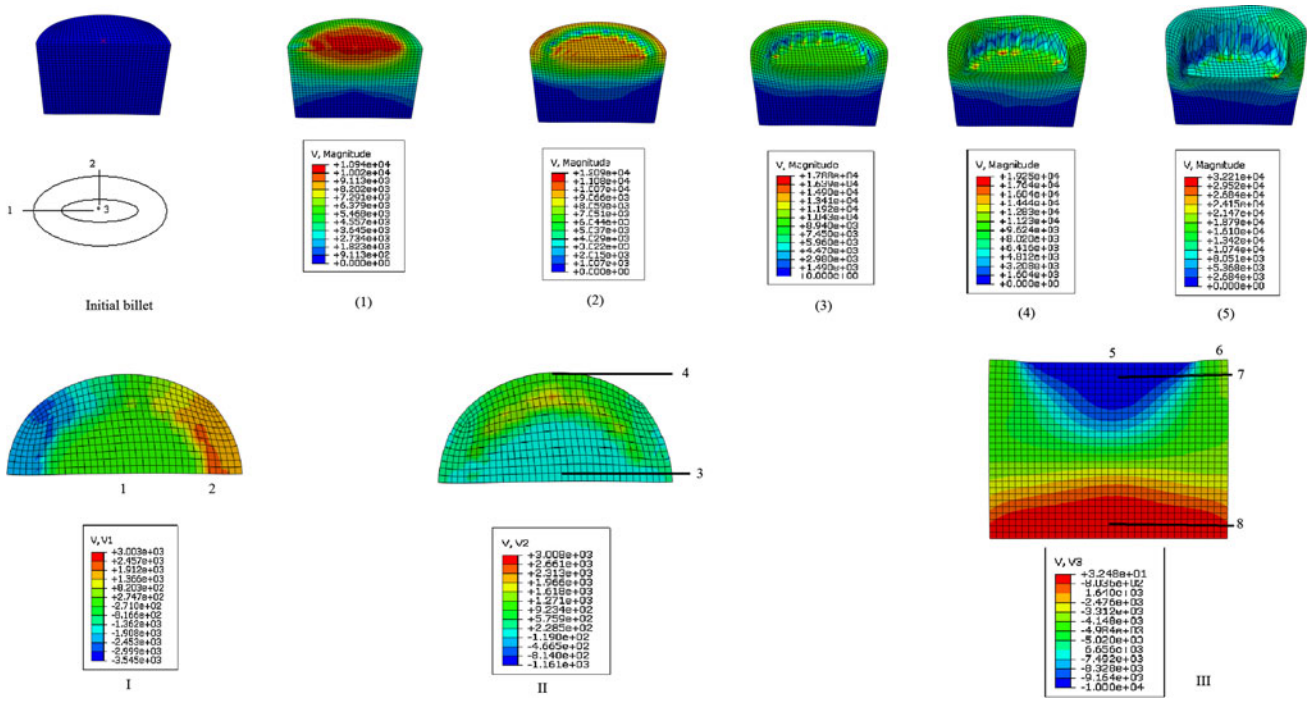

Fig. 18 Results of FEM simulation for spatial velocity at nodes in backward extrusion process of internally elliptic-shaped sections from elliptic billets, RA = 49%, m = 0.1

4. Conclusions

Finite element simulation of the backward extrusion process was carried out for the internally circular and elliptical and externally polygonal, rectangular, and elliptical sections.

The results for rectangular, hexagonal, and octagonal sections achieved from 3D simulations showed good agreement with previous works.

The 3D velocity field distribution and the free surface configurations were obtained by this simulation which had not obtained up to now.

The 3D simulation predictions for the extrusion force for lower reduction of areas were closer to experimental observations while for higher reductions they were further apart.

It was concluded from the results given here that hollow sections with large reductions and thin walls are more prone to distortions due to the large differences in the components of velocity in different directions.

A detailed analysis of strain, stress, and velocity field for the backward extrusion of shaped section was presented which assisted a better understanding of the process.

The advantage of using finite element method over theoretical and experimental methods was also illustrated in this article by producing 3D spatial velocity fields, 3D stress and strain distributions, the extruded product free surface configuration, and the influence of various parameters such as friction, aspect ratio, and percentage reduction of area on these results. Analytical methods could hardly produce any of these results in such a depth and clarity. On the other hand using experimental method some of these results such as the grid deformation could be obtained but not for any arbitrary plane as is the case for the FEM simulation, while other results produced by the simulation could hardly be obtained by the experimental methods which consume a lot of time and money.

References

1. W.B. Bae and D.Y. Yang, An Upper-Bound Analysis of the Backward Extrusion of Internally Elliptic-Shaped Tubes from Round Billets, *J. Mater. Process. Technol.*, 1992, **30**, p 13–20
2. W.B. Bae and D.Y. Yang, An Analysis of Backward Extrusion of Internally Circular Shaped Tubes from Arbitrarily Shaped Billets by the Upper-Bound Method, *J. Mater. Process. Technol.*, 1993, **36**, p 175–185
3. W.B. Bae and D.Y. Yang, An Upper-Bound Analysis of the Backward Extrusion of Tubes of Complicated Internal Shapes from Round Billets, *J. Mater. Process. Technol.*, 1993, **36**, p 157–173
4. R.-S. Lee and C.-T. Kwan, A Modified Analysis of the Backward Extrusion of Internally Circular-Shaped Tubes from Arbitrarily Shaped Billets by the Upper-Bound Elemental Technique, *J. Mater. Process. Technol.*, 1996, **59**, p 351–358
5. Y.T. Lin and J.P. Wang, A New Upper-Bound Elemental Technique Approach, *J. Comput. Struct.*, 1997, **65**(4), p 601–611
6. M.M. Moshksar and R. Ebrahimi, An Analytical Approach for Backward Extrusion Forging of Regular Polygonal Hollow Components, *Int. J. Mech. Sci.*, 1998, **40**(12), p 1247–1263
7. Y.M. Guo, Y. Yokouchi, and K. Nakanishi, Hot Backward Extrusion Comparative Analyses by a Combined Finite Element Method, *Int. J. Mech. Sci.*, 2000, **42**, p 1867–1885
8. K. Abrinia and S. Orangi, A Finite Element Simulation for the Backward Extrusion of Internally Hollow Circular Sections from Polygonal Billets, *J. Coll. Eng. (special issue on: Mech. Eng.) University of Tehran*, 2007, **40**(6), p 771–780
9. K. Abrinia and S. Orangi, A Finite Element Analysis and Process Simulation of Backward Extrusion, *Proceeding of the International Conference on Recent Advances in Mechanical & Materials Engineering*, 30-31 May 2005, Kuala Lumpur, Malaysia
10. S. Orangi and K. Abrinia, 3D Simulation of Backward Extrusion Process for Production of Internally Shaped Circular Tubes Sections from Arbitrarily Shaped Tubes, *International Conference on Mechanical Engineering Conference, Isfahan*, University of technology, Isfahan, Iran, May 2005 (in Farsi)
11. K. Abrinia and S. Orangi, Investigation of Process Parameters for the Backward Extrusion of Arbitrary-Shaped Tubes from Round Billets Using Finite Element Analysis, *J. Mater. Eng. Perform.*, 2009, **18**, p 1201–1208